ORNL/TM-2024/3354

# Developing a Database of Bio-based Materials for Building Envelope Applications


Rui Zhang
Mengjia Tang
Emishaw Iffa
André Desjarlais

**May 2024**

OAK RIDGE National Laboratory

ORNL IS MANAGED BY UT-BATTELLE LLC FOR THE US DEPARTMENT OF ENERGY

**ORNL/TM-2024/3354**

Buildings and Transportation Science Division

# DEVELOPING A DATABASE OF BIO-BASED MATERIALS FOR BUILDING ENVELOPE APPLICATIONS

Rui Zhang
Mengjia Tang
Emishaw Iffa
André Desjarlais

May 2024

Prepared by
OAK RIDGE NATIONAL LABORATORY
Oak Ridge, TN 37831
managed by
UT-BATTELLE LLC
for the
US DEPARTMENT OF ENERGY
under contract DE-AC05-00OR22725

**CONTENTS**

## ABSTRACT

Oak Ridge National Laboratory (ORNL) has been funded by the Department of Energy (DOE) to help accelerate the introduction of building envelope materials that would reduce the carbon footprint of the buildings sector. The DOE's Building Technologies Office has historically sought to resolve the knowledge gaps regarding the energy efficiency and moisture durability of building envelope systems and to develop the data, guidance, and tools needed to facilitate rapid industry adoption of high-performance, moisture-managed envelope systems. This project will help accelerate the widespread acceptance of a new generation of building materials developed specifically with the intent of reducing the carbon footprint of buildings.

We have produced a database of hygrothermal transport properties on low embodied carbon building materials that can be added to energy and durability simulation tools. Properties that were measured include density, heat capacity, thermal conductivity as a function of temperature and relative humidity, moisture dependent permeance, and sorption isotherms as a function of relative humidity. These data sets were measured following consensus national standards using state-of-the-art facilities.

The data has been compiled and is being made available to building designers who require these data to assess these new materials in their designs. We will publish the data and seek its addition to reference databases such as the ASHRAE Handbook of Fundamentals.



## ACKNOWLEDGEMENTS

This work was supported by the Building Technologies Office of the U. S. Department of Energy under Contract No. DE-AC05- 00OR22725 with UT-Battelle, LLC. The authors would like to thank the DOE's Sven Mumme for his support of this project. We are grateful to Graham Wright, Katrin Klingenberg, and Michael Franco of the Passive House Institute US, Inc. (PHIUS) for their efforts and support in identifying materials for evaluation. We also thank Denise Antunes de Silva of ORNL for helping procure some of the materials analyzed in this project and Gunnar Johnson and Islam Safir of ORNL for helping with the laboratory measurements.

## LIST OF FIGURES

## LIST OF TABLES

# 1. BACKGROUND AND OBJECTIVE

Under the 2015 Paris Climate Agreement, parties committed to reducing greenhouse gas (GHG) emissions in response to the pressing climate change challenge (UNFCCC, 2015). It is widely recognized that the building sector plays a substantial role in greenhouse gas (GHG) emissions, accounting for 40% of the total global $CO_2$ emissions each year. Materials used in infrastructure and buildings account for 13% of those overall emissions (Architecture, 2030). These concerning numbers emphasize the importance of reevaluating the approach to managing building materials and their impact on carbon emissions.

To address these concerns, promoting the use of eco-friendly or bio-based building materials is crucial, as evidenced by the severity of the situation. These materials are natural, renewable, and sustainable. This strategic aim aligns with the urgent need to rapidly decrease the amount of carbon emissions that are embedded in materials, thereby offering a practical approach to ultimately eliminate emissions from buildings by 2050.

The objective of this study is to generate a database of bio-based building materials that can be widely used in the energy and durability simulation tools. The study measured density, heat capacity, thermal conductivity as a function of temperature and relative humidity, moisture dependent permeance, and sorption isotherms as a function of relative humidity. The availability of these measured data will accelerate the widespread use of a new generation of building materials designed to minimize the carbon emissions associated with buildings.

# 2. METHODOLOGY

The following sections present material collection and the detailed test methods for evaluating material properties.

## 2.1 MATERIAL COLLECTION

Using the design community as a source of information, this work identified twenty-four bio-based materials that are being marketed for inclusion into building envelopes. The identified materials included claddings, roofing, insulation, sheathings, wall systems, interior finishes, and finished flooring as shown in Figure 1.

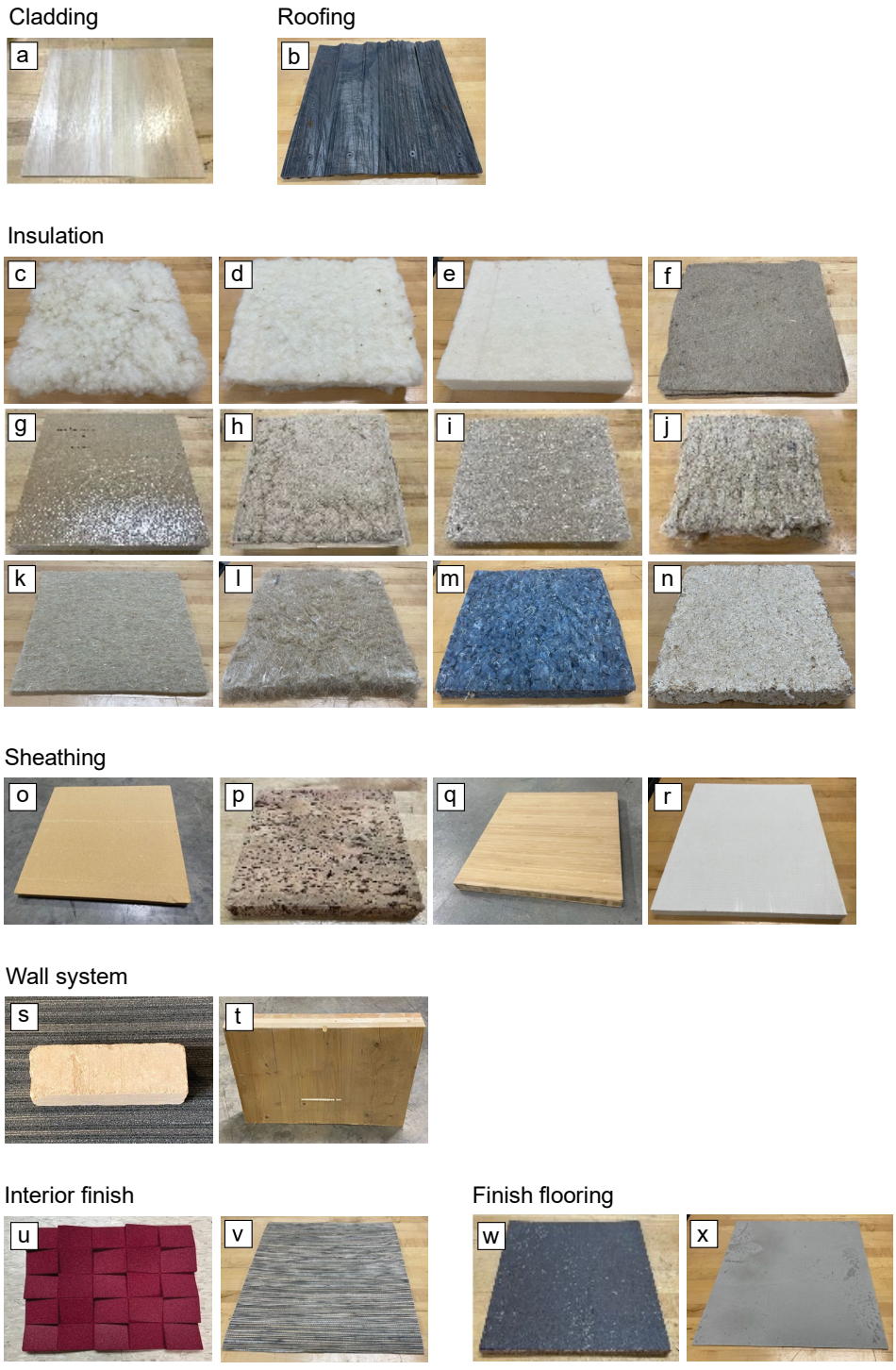


Figure 1. Collected building materials: (a) cedar wood shakes; (b) recycled rubber roof tile; (c) low density sheep wool; (d) medium density sheep wool; (e) high density sheep wool; (f) jute mat; (g) wood fiber sheathing; (h) loose-fill wood fiber; (i) hemp board; (j) hemp batt; (k) high density hemp; (l) low density hemp; (m) blue jeans; (n) mycelium; (o) wood fiber board; (p) cork brick interior cladding; (q) bamboo board; (r) MgO interior sheathing; (s) compressed earth block; (t) cross-laminated timber (CLT); (u) molded cork interior cladding; (v) bamboo wall covering; (w) cork flooring; (x) recycled rubber flooring.

## 2.2 DENSITY MEASUREMENT

The density of each material was measured in accordance with ASTM C303-21*, Standard Test Method for Dimensions and Density of Preformed Block and Board-Type Thermal Insulation*. The materials were resized to a uniform 0.31 m square to fit the dimension of the heat flow meter (HFM) apparatus. After measuring the size and mass of each material, density was calculated by dividing the mass by the volume of the material. For loose-fill materials, they were placed into 0.31 m square empty boxes in order to shape their dimensions to fit the HFM. The thicknesses of these materials in the box were measured before being inserted in HFM. The weights of them were calculated by subtracting the weight of the empty box from the total weight of the filled-material box. The density was then calculated in a manner similar to the other materials.

## 2.3 HEAT CAPACITY MEASUREMENT

Heat capacity was measured using a differential scanning calorimeter (DSC 2500 from TA instruments) shown in Figure 2 in accordance with ASTM E1269-11 (2018), *Standard Test Method for Determining Specific Heat Capacity by Differential Scanning Calorimetry*. Prior to the specific heat capacity measurement, the test specimen was sectioned into a 5 mg portion and sealed in the sample pan with a lid as shown in Figure 2. The temperatures that were chosen to determine the specific heat capacity were 30 °C, 35 °C, 40 °C, 45 °C, 50 °C, 55 °C, 60 °C, 65 °C, 70 °C, and 75 °C. The purge gas during the DSC measurements was nitrogen gas flowing at a rate of 50 ml/min. From the initial to the final temperature, the DSC test chamber was heated at a rate of 20 °C/min. Furthermore, TRIOS software was employed to perform data acquisition and calculations.

(a) (b)

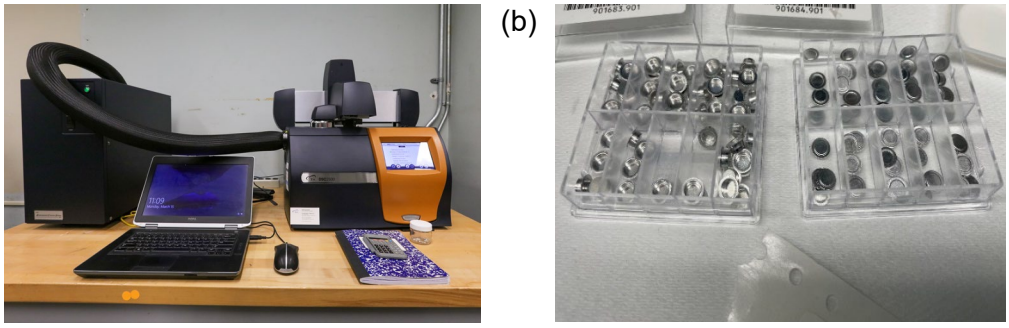

Figure 2. Differential scanning calorimeter (a); sample pan and lid (b).

## 2.4 THERMAL CONDUCTIVITY MEASUREMENT

Thermal conductivity was measured by the HFM apparatus shown in Figure 3 in accordance with ASTM C518-21 (2021), *Standard Test Method for Steady-State Thermal Transmission Properties by Means of the Heat Flow Meter Apparatus*. The HFM (Model 304/305) used for these experiments was manufactured by TA Instruments with a reported 3% measurement error. Prior to the thermal conductivity measurements, rigid materials were cut into 0.31 m × 0.31 m square samples. For loose-fill materials, they were filled into 0.31 m × 0.31 m square empty boxes in order to shape their dimensions to fit the HFM. During the thermal conductivity measurement, the auto thickness mode was set for rigid materials, which measured the distance between the upper and lower plates in the HFM to represent the sample thicknesses; in order to keep original densities of blanket and batt-type materials, the manual thickness mode was set for these materials using their initial thicknesses measured on the bench.

Figure 3. Heat flow meter.

### 2.4.1 Temperature – dependent thermal conductivity

In order to investigate temperature effect on the thermal conductivity, three sets of temperatures were selected in accordance with ASTM C1058-03 (2008), *Standard Practice for Selecting Temperatures for Evaluating and Reporting Thermal Properties of Thermal Insulation*. Upper and lower plate temperatures in the HFM were set at −4 °C /24 °C, 10 °C /38 °C, and 24 °C /52 °C, respectively. These sets created mean temperatures of 10 °C, 24 °C, and 38 °C. Prior to thermal conductivity measurements, the samples were stored at standard laboratory conditions: a temperature of 19 °C and a relative humidity (RH) of 31%. They were then placed between the upper and lower plates of the HFM, and their thermal conductivities were subsequently measured at these three mean temperatures. Thermal equilibrium criteria for the HFM measurements included: 0.2 °C temperature equilibrium, 40 μV between block HFM equilibrium, and 2% HFM change between the neighboring blocks. Each block ran approximately 6 – 7 min.

### 2.4.2 Relative humidity – dependent thermal conductivity

In order to investigate relative humidity effect on the thermal conductivity, three RH levels at a mean temperature 24 °C were chosen: 0%, 50%, and 80%. As shown in Figure 4, samples of each material were stored in the following conditions: a 0% RH oven set at the standard laboratory temperature 19 °C with flushing dry air, a climate chamber controlled at 24 °C and 50% RH, and a second climate chamber controlled at 24 °C and 80% RH. The samples were placed into these conditions for a period of one month in order to guarantee that the moisture adsorption of the samples reached a steady state. The samples were then removed from these conditions and fully covered with plastic wraps to prevent the loss of any moisture adsorbed in the samples. Subsequently, the wrapped samples were positioned between the upper and lower plates of the HFM, and thermal conductivity was then measured at a mean temperature 24 °C with the upper plate set at 10 °C and the lower plate at 38 °C.

(a)  (b) 

Figure 4. Oven (a) and environmental climate chamber (b).

## 2.5 WATER VAPOR TRANSMISSION MEASUREMENT

In order to determine the water vapor transmission rate of materials, measurements were conducted in accordance with ASTM E96-22 (2022), *Standard Test Methods for Gravimetric Determination of Water Vapor Transmission Rate of Materials*. These measurements used the desiccant method (dry cup) and the water method (wet cup) to evaluate the permeabilities of the materials under five average relative humidity levels, i.e., 25%, 41.4%, 62.7%, 71.9% and 86.9% as shown in Table 1. For each average RH level, three samples were used for replicated measurements; in each climate chamber, one blank sample was used to compensate for variability due to fluctuations of temperature and/or barometric pressure. The following will introduce: 1) the methods employed to obtain a constant RH in the test cup; 2) the thermal settings of climate chambers; and 3) the test procedure.

Table 1. Average relative humidity levels for water vapor transmission measurements at 24 °C.

| No. | Desiccant/salt solution in the test cup | RH in the test cup | RH in the chamber | Average RH |
|---|---|---|---|---|
| 1 | $CaCl_2$ | 0% | 50% | 25% |
| 2 | $MgCl_2$ | 32.9% | 50% | 41.4% |
| 3 | NaCl | 75.3% | 50% | 62.7% |
| 4 | $KNO_3$ | 93.8% | 50% | 71.9% |
| 5 | $KNO_3$ | 93.8% | 80% | 86.9% |

In order to maintain constant RH in test cups, different salts were selected for making aqueous solutions in accordance with ASTM E104, *Standard Practice for Maintaining Constant Relative Humidity by Means of Aqueous Solutions*. The desiccant and salts that were chosen are described as follows:

- For the desiccant method (dry cup), anhydrous calcium chloride ($CaCl_2$) was used in the cup with a relative humidity of 0%.

- For the water method (wet cup), three saturated salt solutions in the cup were employed, including magnesium chloride ($MgCl_2$), sodium chloride (NaCl), and potassium nitrate ($KNO_3$) salts. The equilibrium relative humidities of the selected saturated salt solutions at 24 °C were as follows: 33.1% for magnesium chloride, 75% for sodium chloride, and 94.6% for potassium nitrate, respectively.

In order to obtain different RHs for each material, the samples with different RH cups were placed within two climate chambers as shown in Figure 5. Both chambers had controlled temperature and relative humidity: one was maintained at 24 °C and 50% RH, another was at 24 °C and 80% RH.

Figure 5. Test samples in the environmental climate chamber at 24 °C and 50% RH.

Prior to the measurements, the rigid materials were cut into disk samples with a 0.152 m diameter. For loose-fill materials, these materials were placed into cylindrical PVC holders with a 0.152m inner diameter. The bottom of the holders was sealed with the mesh grid to hold the materials and allow the water vapor to transfer through it. Following the sample preparation, as illustrated in Figure 6, the cup was filled with the proper amount of desiccant/salt solutions to have approximately 12 mm of air space between the desiccant/salt solution and the sample; and the sample with/without a grid PVC holder was then placed on the top of the cup with a wax sealing for the rigid sample's edge and a tape sealing for the loose-fill sample's holder edge. Once the samples were weighed, they were placed into the climate chambers. The cup was weighed periodically: once a day for rigid samples and twice a day for loose-fill samples, until the rate of weight change of the sample reached a steady state with the rate being essentially constant over a period. After identifying the steady state portion of the test, the water vapor permeability was calculated based on the Eq.1 - 3.

$$WVTR = \frac{G}{t \cdot A} \tag{1}$$

$$WVP = \frac{WVTR}{\Delta p} = \frac{WVTR}{S \cdot (R_1 - R_2)} \tag{2}$$

$$Permeability = WVP \cdot thickness \tag{3}$$

where:
$WVTR$ = water vapor transmission rate, g/h·m$^2$,
$G$ = steady state weight change, g,
$t$ = time, h,

$A$ = test area, $m^2$,
$WVP$ = water vapor permeance, ng/(Pa·s·$m^2$),
$\Delta p$ = vapor pressure difference, Pa,
$S$ = saturation vapor pressure at test temperature, Pa,
$R_1$ = relative humidity at the source expressed as a fraction,
$R_2$ = relative humidity at the vapor sink expressed as a fraction,
$Permeability$ = water vapor permeability, ng/(Pa·s·m), and
$thickness$ = sample thickness, m.

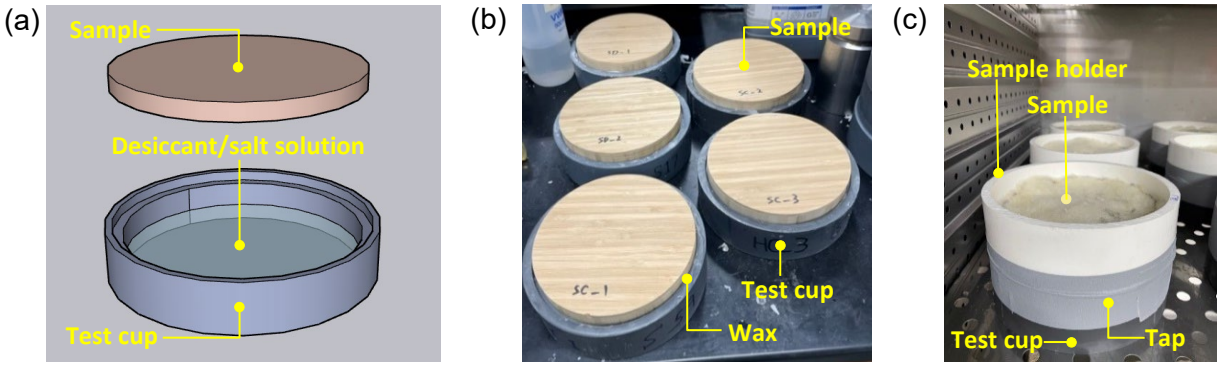


Figure 6. Test cup with the desiccant/salt solution (a), waxed samples (b), and tape-sealed samples (c).

## 2.6 SORPTION ISOTHERM MEASUREMENT

### 2.6.1 Hygroscopic adsorption isotherm test

The adsorption isotherm tests were conducted in desiccators with saturated salt solutions according to ASTM C1498-04a (2016), *Standard Test Method for Hygroscopic Sorption Isotherms of Building Materials*. Three salt solutions – magnesium chloride ($MgCl_2$), sodium chloride (NaCl), and potassium nitrate ($KNO_3$) – were prepared by dissolving slightly excessive masses of ACS reagent grade or high purity grade salts into 600 ml distilled water. The equilibrium relative humidity in the air space above the saturated salt solutions at 24 °C is shown in Table 2 after a linear interpolation between neighboring temperatures according to ASTM E104-20a (2020), *Standard Practice for Maintaining Constant Relative Humidity by Means of Aqueous Solutions*. Temperature/relative humidity data loggers (HOBO®, MX1101) were placed on the perforated ceramic plate above each salt solution to check the equilibrium relative humidity. The desiccators were placed in two environment chambers (BINDER, KMF 720) with a temperature of 24 ± 0.5 °C and relative humidity of 50% ± 2% or 80% ± 2%.

Table 2. Saturated aqueous salt solutions and corresponding equilibrium relative humidity at 24 °C.

| Salt solution | RH |
|---|---|
| $MgCl_2$ | 32.9% |
| NaCl | 75.3% |
| $KNO_3$ | 93.8% |

For each material, three specimens with ≥10 g mass were cut into small pieces at a length scale of 25 mm and placed in an oven for at least 5 days. The three materials that were first tested (i.e., cork brick interior cladding, bamboo board, and wood fiber sheathing) were dried at 100 °C, but all the materials tested afterwards were dried at 50 °C to prevent melting. After drying, the specimens were moved from the oven to weighing cups, cooled down to room temperature inside closed weighing cups, and then weighed using a mass comparator (METTLER TOLEDO, PR5003, 0.001 g resolution) to obtain the dry mass. The weighing cups with the specimens were placed inside the desiccators with saturated salt solutions, with the lids open and put beside the weighing cups (Figure 7). Each specimen was subject to one RH level instead of a series of RH levels so that tests under different RH levels can be conducted simultaneously in order to accelerate the determination of water sorption isotherms. All materials were tested in triplicates.


Figure 7. Photos of (a) specimens in three desiccators with three saturated salt solutions and (b) specimens in open weighing cups during an adsorption test.

The specimens were weighed every day at an interval of approximately 24 h whenever possible. For each weighing, the weighing cups were closed with the lid, weighed, and placed back to the original desiccators with the lid beside them. This process was repeated until the daily weighing difference relative to the previous day was within 0.1% for three successive days.

The specimen mass on the last day was used to compute the equilibrium moisture content at the specific RH ((4):

$$EMC_{x\%\,RH} = \frac{M_{x\%\,RH} - M_{0\%\,RH}}{M_{0\%\,RH}} \times 100\% \quad (4)$$

Where $EMC_{x\%\,RH}$ represents the equilibrium moisture content at $x\%\ RH$, unitless; $M_{x\%\,RH}$ represents the specimen mass on the last day at $x\%\ RH$, g; $M_{0\%\,RH}$ represents the dry mass of the specimen, g.

### 2.6.2 Free saturation test

The three materials that were first tested (i.e., cork brick interior cladding, bamboo board, and wood fiber sheathing) were cut into 51 mm × 51 mm pieces, dried in the oven at 100 °C, weighed to obtain the dry mass, and then immersed in distilled water. Each specimen contained one piece of the material, which led to a dry mass of approximately 5 g, 29 g, and 18 g for the cork brick interior cladding, bamboo board, and wood fiber sheathing, respectively. The other materials tested later were cut into around 25 mm × 25 mm pieces and dried in the oven at 50 °C. Then 10 – 20 g of the dried material were moved into weighing cups and weighed to obtain the dry mass. Afterwards, the specimens were transferred into a PVC pipe (127 mm in diameter and 102 mm in height) which were sealed with metal mesh on two ends. After the PVC pipes with the specimens inside were weighed, they were immersed in distilled water (Figure 8).

The PVC pipe and metal mesh were used to prevent mass loss due to material disintegration in water. All materials were tested in triplicates.

Figure 8. Specimens inside PVC pipes during a free saturation test.

The specimens were weighed daily with an approximately 24 h interval at the beginning of a test, and the weighing frequency was decreased to three times or twice a week later when the increase in mass became slow. For materials that were immersed by themselves (i.e., cork brick interior cladding, bamboo board, and wood fiber sheathing), the specimens were taken out of water, allowed to drip liquid water in the air, weighed, and placed back into water. For materials that were inside PVC pipes, the PVC pipes were taken out of water and allowed to drip liquid water in the air, then the exterior surface of the PVC pipes and the two mesh surfaces were wiped with dry paper towels before weighing. The test was completed when the mass increase rate for most materials was $\leq 0.1$ g/day for the last 21 days or when 100 days was reached. The value of 0.1 g/day was selected here because blotting softwood specimens caused a repeatability error of $\pm$ 0.1 g (Glass et al., 2024). For several highly porous materials tested in this study (i.e., mycelium, recycled blue jeans, loose-fill wood fiber, medium density sheep wool, and high-density sheep wool), the repeatability error was much higher than $\pm$ 0.1 g because of the large pores on exterior surfaces. Therefore, the equilibrium criterion for them was $\leq 0.5$ g/day for the last 21 days. The equilibrium moisture content was calculated in the same way as adsorption isotherm tests.

# 3. RESULTS

## 3.1 DENSITY

The densities of collected bio-based materials measured are listed in Table 3. The density range varies from 8 kg/m$^3$ (low density sheep wool) to 1907 kg/m$^3$ (compressed earth block).

Table 3. Dry density of building materials.

| No. | Material | Thickness [mm] | Density [kg/m³] |
|---|---|---|---|
| 1 | Wood fiber sheathing | 40 | 236 |
| 2 | Loose-fill wood fiber | 57 | 78 |
| 3 | Wood fiber board | 42 | 131 |
| 4 | Cross-laminated timber | 98 | 521 |
| 5 | Cedar wood shakes | 14 | 273 |
| 6 | Cork flooring | 7 | 940 |
| 7 | Molded cork interior cladding | 24 | 225 |
| 8 | Cork brick interior cladding | 13 | 256 |
| 9 | Bamboo wall covering | 1 | 190 |
| 10 | Bamboo board | 19 | 660 |
| 11 | High density hemp | 10 | 60 |
| 12 | Low density hemp | 25 | 27 |
| 13 | Hemp batt | 650 | 32 |
| 14 | Hemp board | 52 | 95 |
| 15 | Low density sheep wool | 52 | 8 |
| 16 | Medium density sheep wool | 59 | 21 |
| 17 | High density sheep wool | 64 | 31 |
| 18 | Recycled rubber flooring | 2 | 1276 |
| 19 | Recycled rubber roof tile | 3 | 1167 |
| 20 | Compressed earth block | 91 | 1907 |
| 21 | MgO interior sheathing | 20 | 927 |
| 22 | Recycled blue jeans | 31 | 48 |
| 23 | Jute mat | 14 | 96 |
| 24 | Mycelium | 37 | 123 |

### 3.2 HEAT CAPACITY

Table 4 shows the measured heat capacity for each building material from 30 °C to 75 °C. The range of the heat capacity was from 0.56 to 3.36 J/(g·°C). With increasing the temperature, the heat capacity increased.

Table 4. Heat capacity results.

| No. | Material | Heat capacity at different temperatures, [J/(g·°C)] | | | | | | | | | |
|---|---|---|---|---|---|---|---|---|---|---|---|
| | | 30 °C | 35 °C | 40 °C | 45 °C | 50 °C | 55 °C | 60 °C | 65 °C | 70 °C | 75 °C |
| 1 | Wood fiber sheathing | 1.97 | 2.05 | 2.16 | 2.27 | 2.38 | 2.47 | 2.55 | 2.67 | 2.81 | 2.97 |
| 2 | Loose-fill wood fiber | 1.77 | 1.95 | 2.19 | 2.46 | 2.77 | 3.11 | 3.50 | 3.89 | 4.25 | 4.53 |
| 3 | Wood fiber board | 1.82 | 1.89 | 1.99 | 2.11 | 2.24 | 2.34 | 2.45 | 2.55 | 2.64 | 2.71 |
| 4 | Cross-laminated timber | 1.93 | 1.99 | 2.06 | 2.12 | 2.20 | 2.27 | 2.34 | 2.40 | 2.43 | 2.46 |
| 5 | Cedar wood shakes | 2.01 | 2.09 | 2.19 | 2.30 | 2.42 | 2.57 | 2.73 | 2.91 | 3.10 | 3.30 |
| 6 | Cork flooring | 1.38 | 1.50 | 1.59 | 1.70 | 1.80 | 1.86 | 1.92 | 2.00 | 2.07 | 2.11 |
| 7 | Molded cork interior cladding | 2.11 | 2.18 | 2.27 | 2.37 | 2.50 | 2.68 | 2.90 | 2.95 | 2.94 | 2.89 |
| 8 | Cork brick interior cladding | 1.81 | 1.90 | 2.00 | 2.11 | 2.24 | 2.33 | 2.47 | 2.69 | 2.98 | 3.21 |
| 9 | Bamboo wall covering | 1.60 | 1.64 | 1.69 | 1.75 | 1.82 | 1.89 | 1.98 | 2.06 | 2.15 | 2.25 |
| 10 | Bamboo board | 1.63 | 1.67 | 1.72 | 1.77 | 1.82 | 1.87 | 1.91 | 1.95 | 1.98 | 2.01 |
| 11 | High density hemp | 0.65 | 0.75 | 0.82 | 0.89 | 0.99 | 1.08 | 1.21 | 1.35 | 1.51 | 1.66 |
| 12 | Low density hemp | 1.31 | 1.36 | 1.41 | 1.47 | 1.54 | 1.61 | 1.70 | 1.85 | 1.91 | 2.02 |
| 13 | Hemp batt | 0.74 | 0.81 | 0.87 | 0.93 | 1.00 | 1.04 | 1.10 | 1.17 | 1.20 | 1.23 |
| 14 | Hemp board | 1.54 | 1.57 | 1.63 | 1.70 | 1.77 | 1.83 | 1.90 | 2.00 | 2.02 | 2.05 |
| 15 | Low density sheep wool | 1.81 | 1.86 | 1.93 | 2.00 | 2.09 | 2.20 | 2.31 | 2.43 | 2.58 | 2.74 |
| 16 | Medium density sheep wool | 1.78 | 1.84 | 1.92 | 2.01 | 2.11 | 2.23 | 2.36 | 2.51 | 2.68 | 2.88 |
| 17 | High density sheep wool | 1.59 | 1.71 | 1.84 | 1.99 | 2.18 | 2.38 | 2.61 | 2.87 | 3.12 | 3.36 |
| 18 | Recycled rubber flooring | 0.56 | 0.64 | 0.67 | 0.69 | 0.71 | 0.73 | 0.74 | 0.76 | 0.77 | 0.79 |
| 19 | Recycled rubber roof tile | 1.64 | 1.75 | 1.87 | 1.89 | 1.92 | 1.99 | 2.04 | 2.10 | 2.17 | 2.23 |
| 20 | Compressed earth block | 0.98 | 0.99 | 1.00 | 1.02 | 1.03 | 1.04 | 1.05 | 1.07 | 1.08 | 1.09 |
| 21 | MgO interior sheathing | 1.36 | 1.40 | 1.43 | 1.46 | 1.49 | 1.52 | 1.55 | 1.57 | 1.60 | 1.64 |
| 22 | Recycled blue jeans | 1.21 | 1.24 | 1.27 | 1.31 | 1.34 | 1.38 | 1.46 | 1.48 | 1.50 | 1.52 |
| 23 | Jute mat | 1.84 | 1.92 | 2.02 | 2.11 | 2.20 | 2.31 | 2.43 | 2.54 | 2.69 | 2.87 |
| 24 | Mycelium | 1.66 | 1.69 | 1.74 | 1.80 | 1.86 | 1.92 | 1.97 | 2.01 | 2.04 | 2.07 |

## 3.3 THERMAL CONDUCTIVITY

### 3.3.1 Results for temperature – dependent thermal conductivity

Table 5 presents the measured thermal conductivity at different temperatures for each material. For most of materials, increasing the temperature from 10 °C to 38 °C elevated their thermal conductivities except for bamboo board, recycled rubber flooring, and MgO interior sheathing.

Table 5. Measured thermal conductivity at different temperatures.

| No. | Material | Thermal conductivity at different temperatures, [W/(m·K)] | | |
|---|---|---|---|---|
| | | 10 °C | 24 °C | 38 °C |
| 1 | Wood fiber sheathing | 0.052 | 0.053 | 0.054 |
| 2 | Loose-fill wood fiber | 0.046 | 0.048 | 0.050 |
| 3 | Wood fiber board | 0.042 | 0.042 | 0.045 |
| 4 | Cross-laminated timber | 0.127 | 0.130 | 0.134 |
| 5 | Cedar wood shakes | 0.066 | 0.069 | 0.072 |
| 6 | Cork flooring* | 0.061 | 0.060 | 0.058 |
| 7 | Molded cork interior cladding* | 0.054 | 0.056 | 0.060 |
| 8 | Cork brick interior cladding | 0.043 | 0.044 | 0.046 |
| 9 | Bamboo wall covering* | 0.039 | 0.041 | 0.044 |
| 10 | Bamboo board | 0.161 | 0.158 | 0.155 |
| 11 | High density hemp | 0.034 | 0.036 | 0.038 |
| 12 | Low density hemp | 0.045 | 0.049 | 0.053 |
| 13 | Hemp batt | 0.043 | 0.045 | 0.046 |
| 14 | Hemp board | 0.045 | 0.047 | 0.048 |
| 15 | Low density sheep wool | 0.063 | 0.070 | 0.078 |
| 16 | Medium density sheep wool | 0.040 | 0.042 | 0.045 |
| 17 | High density sheep wool | 0.035 | 0.037 | 0.039 |
| 18 | Recycled rubber flooring* | 0.256 | 0.251 | 0.245 |
| 19 | Recycled rubber roof tile* | 0.131 | 0.157 | 0.204 |
| 20 | Compressed earth block | 0.449 | 0.470 | 0.490 |
| 21 | MgO interior sheathing | 0.171 | 0.168 | 0.164 |
| 22 | Recycled blue jeans | 0.035 | 0.037 | 0.039 |
| 23 | Jute mat | 0.041 | 0.043 | 0.044 |
| 24 | Mycelium | 0.051 | 0.053 | 0.055 |

* These materials were stacked with 25 mm thick foam insulation for measuring their thermal conductivities.

### 3.3.2 Results for relative humidity – dependent thermal conductivity

Table 6 presents the measured thermal conductivity at different relative humidity levels and 24 °C for each material. The thermal conductivities of the samples increased slightly as RH increased, with the exception of the MgO interior cladding, which had a decrease in thermal conductivity.

Table 6. Measured thermal conductivity at different relative humidity levels.

| No. | Material | Thermal conductivity at 24 °C [W/(m·K)] | | |
|---|---|---|---|---|
| | | 0% RH | 50% RH | 80% RH |
| 1 | Wood fiber sheathing | 0.049 | 0.054 | 0.056 |
| 2 | Loose-fill wood fiber | 0.042 | 0.046 | 0.057 |
| 3 | Wood fiber board | 0.039 | 0.042 | 0.050 |
| 4 | Cross-laminated timber | N/A | N/A | N/A |
| 5 | Cedar wood shakes | 0.066 | 0.071 | 0.069 |
| 6 | Cork flooring* | 0.089 | 0.105 | 0.104 |
| 7 | Molded cork interior cladding* | 0.052 | 0.056 | 0.055 |
| 8 | Cork brick interior cladding | 0.041 | 0.043 | 0.043 |
| 9 | Bamboo wall covering* | 0.050 | 0.043 | 0.042 |
| 10 | Bamboo board | 0.119 | 0.150 | 0.155 |
| 11 | High density hemp | 0.037 | 0.037 | 0.037 |
| 12 | Low density hemp | 0.050 | 0.050 | 0.049 |
| 13 | Hemp batt | 0.044 | 0.046 | 0.049 |
| 14 | Hemp board | 0.042 | 0.044 | 0.050 |
| 15 | Low density sheep wool | 0.063 | 0.065 | 0.065 |
| 16 | Medium density sheep wool | 0.043 | 0.044 | 0.043 |
| 17 | High density sheep wool | 0.037 | 0.038 | 0.039 |
| 18 | Recycled rubber flooring* | 0.099 | 0.129 | 0.134 |
| 19 | Recycled rubber roof tile* | 0.093 | 0.101 | 0.115 |
| 20 | Compressed earth block | N/A | N/A | N/A |
| 21 | MgO interior sheathing | 0.176 | 0.173 | 0.169 |
| 22 | Recycled blue jeans | 0.037 | 0.037 | 0.038 |
| 23 | Jute mat | 0.040 | 0.041 | 0.043 |
| 24 | Mycelium | 0.050 | 0.055 | 0.059 |

N/A: no measurement data due to the inability to fabricate an appropriate sample.
* These materials were stacked with 25 mm thick foam insulation for measuring their thermal conductivities.

### 3.4 WATER VAPOR TRANSMISSION

Table 7 shows the measured water vapor permeability at different relative humidity levels from 25% to 87%. For the measured bio-based building materials, the range of water vapor permeability was between 0.06 ng/(Pa·s·m) and 1054.62 ng/(Pa·s·m). Among these materials, high density hemp, low density hemp, hemp batt, low density sheep wool and medium density sheep wool were very permeable with higher permeability than 51 ng/(Pa·s·m).

Table 7. Measured water vapor permeability at different relative humidity levels.

| No. | Material | Thickness [mm] | Water vapor permeability [ng/(Pa·s·m)] | | | | |
|---|---|---|---|---|---|---|---|
| | | | 25% RH | 41% RH | 63% RH | 72% RH | 87% RH |
| 1 | Wood fiber sheathing | 19 | 3.3 | 5.5 | 6.6 | 6.0 | 23.1 |
| 2 | Loose-fill wood fiber | N/A | N/A | N/A | N/A | N/A | N/A |
| 3 | Wood fiber board | 17 | 36.4 | 137 | 109 | 100 | 204 |
| 4 | Cross-laminated timber | 12 | 0.57 | 1.2 | 1.9 | 3.2 | 22.6 |
| 5 | Cedar wood shakes | 10 | 0.46 | 2.0 | 2.3 | 8.0 | 42.7 |
| 6 | Cork flooring | 7 | 0.06 | 0.27 | 0.35 | 0.96 | 0.85 |
| 7 | Molded cork interior cladding | 6 | 3.9 | 4.3 | 4.7 | 4.4 | 6.2 |
| 8 | Cork brick interior cladding | 7 | 5.5 | 8.0 | 6.4 | 5.3 | 5.5 |
| 9 | Bamboo wall covering | 2 | 1.5 | 4.2 | 13.5 | 21.4 | 31.0 |
| 10 | Bamboo board | 19 | 0.22 | 0.64 | 0.83 | 1.5 | 10.0 |
| 11 | High density hemp | 13 | 62 | 109 | 190 | 210 | 735 |
| 12 | Low density hemp | 51 | 98.6 | 227 | 295 | 252 | 1055 |
| 13 | Hemp batt | 51 | 108 | 225 | 230 | 345 | 584 |
| 14 | Hemp board | 29 | 51.1 | 137 | 164 | 168 | 315 |
| 15 | Low density sheep wool | 51 | 249 | 461 | 579 | 622 | 676 |
| 16 | Medium density sheep wool | 33 | 98.1 | 166 | 180 | 205 | 277 |
| 17 | High density sheep wool | 27 | 49.0 | 128 | 135 | 129 | 335 |
| 18 | Recycled rubber flooring | 2 | 1.6 | 2.1 | 2.3 | 2.5 | 4.9 |
| 19 | Recycled rubber roof tile* | - | - | - | - | - | - |
| 20 | Compressed earth block | N/A | N/A | N/A | N/A | N/A | N/A |
| 21 | MgO interior sheathing | 20 | 5.2 | 9.0 | 9.8 | 9.8 | 17.4 |
| 22 | Recycled blue jeans | N/A | N/A | N/A | N/A | N/A | N/A |
| 23 | Jute mat | 3 | 28.6 | 69.0 | 66.0 | 86.4 | 607 |
| 24 | Mycelium | N/A | N/A | N/A | N/A | N/A | N/A |

N/A: no measurement data due to the inability to fabricate an appropriate sample.
*: Material is impermeable.

## 3.5 SORPTION ISOTHERM

### 3.5.1 Temporal change of specimen mass during hygroscopic adsorption

Figure 9 shows the daily mass change of mycelium and MgO at 93.8% RH. The three MgO specimens reached ≤ 0.1% relative increase in mass on Day 27 and satisfied the equilibrium criteria on Day 29. The tests of three mycelium specimens were stopped prematurely due to signs of mold forming on them.

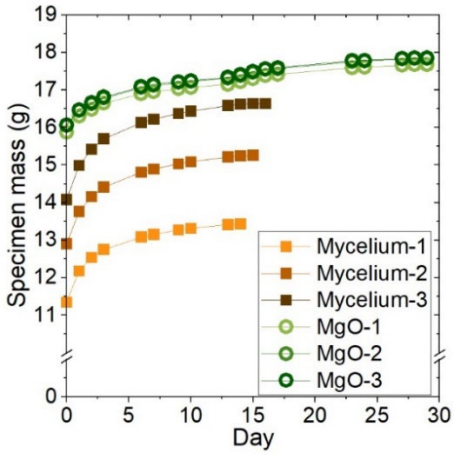


Figure 9. Daily mass change of mycelium and MgO at 93.8% RH. The number 1 – 3 indicates the three replicates of the same material.

### 3.5.2 Temporal change of specimen mass during free saturation

Figure 10 shows the daily mass change of mycelium, MgO, jute mat, and blue jeans during the free saturation test. The fluctuations in the mass of mycelium, jute mat, and blue jeans are clear due to difficulty with consistently removing free liquid water from specimens' exterior surfaces before weighing. However, it is still reasonable to assume that equilibrium was reached for these materials by the end of the test because there was no obvious trend of increase or decrease when looking at a time frame of 21 days.

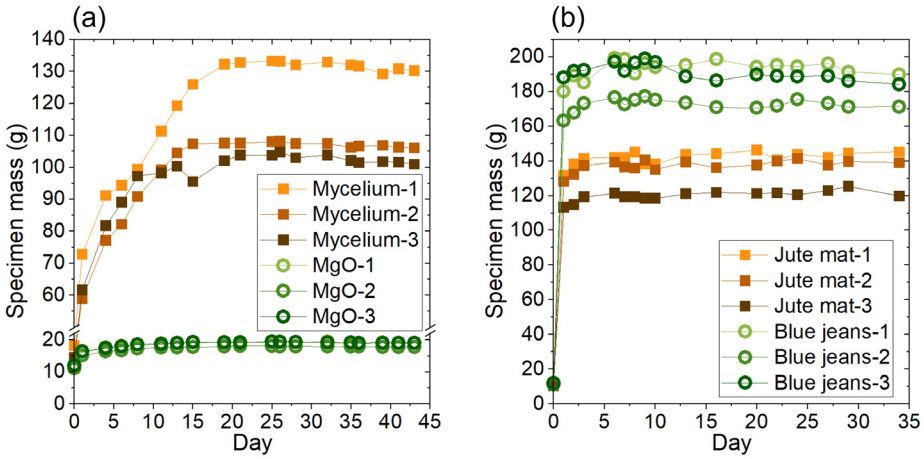


Figure 10. Daily mass change of (a) mycelium and MgO and (b) jute mat and blue jeans during the free saturation test. The number 1 – 3 indicates the three replicates of the same material.

### 3.5.3 Mold growth

Mold started to grow on mycelium, bamboo wall covering, and wood fiber board after 14 days, 17 days, and 30 days, respectively, at 93.8% RH. The photos are shown in Figure 11. Because the bio-based materials can provide nutrients for mold, mold can grow when RH is high. Therefore, it is important to treat bio-based materials with biocides to prevent mold growth when applying them in buildings.

(a) Mycelium


(b) Bamboo wall covering

(c) Wood fiber board

Figure 11. Photos of mold on (a) mycelium, (b) bamboo wall covering, and (c) wood fiber board at 93.8% RH.

### 3.5.4 Equilibrium moisture content

The equilibrium moisture content of 24 materials at 32.9%, 75.3%, 93.8%, and 100% RH is summarized in Table 8 as the average of triplicates for each material. The water sorption property varied by the base material and structure of the material. Amongst base materials, wood fiber, wood, bamboo, hemp, sheep wool, jute, and mycelium adsorbed more water vapor than cork, rubber, earth, magnesium oxide, and cotton within the range of 32.9% – 93.8% RH. Sheep wool is the most adsorptive material, while rubber is the least. Materials made from the same base may differ in the equilibrium moisture content; examples include the cork flooring vs. cork brick interior cladding, bamboo board vs. bamboo wall covering, high density sheep wool vs. low density sheep wool, and wood fiber board vs. loose-fill wood fiber. During the free saturation test at 100% RH, capillary absorption happened in all the pores of the materials. Recycled blue jeans, loose-fill wood fiber, high density sheep wool, and hemp batt absorbed the most liquid water and thus are the most porous.

Table 8. The average of equilibrium moisture content (weight %) at 32.9%, 75.3%, 93.8%, and 100% RH.

| No. | Material | 32.9% RH | 75.3% RH | 93.8% RH | 100% RH |
|---|---|---|---|---|---|
| 1 | Wood fiber sheathing | 4.17 | 9.41 | 12.9 | 376* |
| 2 | Loose-fill wood fiber | 3.96 | 12.0 | 22.4 | 1.39e3 |
| 3 | Wood fiber board | 2.75 | 9.95 | 18.3 | 842 |
| 4 | Cross-laminated timber | 3.63 | 10.6 | 16.2 | 179 |
| 5 | Cedar wood shakes | 3.66 | 10.2 | 16.1 | 284 |
| 6 | Cork flooring | 0.403 | 1.31 | 2.14 | 57.5 |
| 7 | Molded cork interior cladding | 1.21 | 4.37 | 8.56 | 461 |
| 8 | Cork brick interior cladding | 2.12 | 6.47 | 10.9 | 159 |
| 9 | Bamboo wall covering | 3.30 | 12.0 | 21.9 | 568 |
| 10 | Bamboo board | 3.05 | 8.04 | 12.8 | 103 |
| 11 | High density hemp | 3.26 | 8.90 | 16.0 | 770* |
| 12 | Low density hemp | 3.25 | 9.09 | 16.6 | 793 |
| 13 | Hemp batt | 3.09 | 9.05 | 16.3 | 1.32e3 |
| 14 | Hemp board | 2.24 | 8.39 | 19.1 | 826 |
| 15 | Low density sheep wool | 2.49 | 16.2 | 26.9 | 708 |
| 16 | Medium density sheep wool | 4.31 | 15.8 | 28.7 | 1.02e3 |
| 17 | High density sheep wool | 3.20 | 9.02 | 15.1 | 1.35e3 |
| 18 | Recycled rubber flooring | 0.221 | 0.632 | 1.47 | 59.4 |
| 19 | Recycled rubber roof tile | 0.00266 | 0.0240 | 0.0643 | 17.7 |
| 20 | Compressed earth block | 0.393 | 1.37 | 2.41 | 26.0 |
| 21 | MgO interior sheathing | 1.34 | 5.62 | 11.2 | 59.6 |
| 22 | Recycled blue jeans | 1.05 | 3.55 | 6.04 | 1.46e3 |
| 23 | Jute mat | 3.65 | 11.9 | 20.3 | 1.09e3 |
| 24 | Mycelium | 3.87 | 12.1 | 18.3 | 615 |

* Tests were stopped after 100 days, and the sample mass was still increasing or decreasing significantly.

## 4. CONCLUSIONS

This study evaluated 24 bio-based materials including: cedar wood shakes, recycled rubber roof tile, low density sheep wool, medium density sheep wool, high density sheep wool, jute mat, wood fiber sheathing, loose-fill wood fiber, hemp board, hemp batt, high density hemp, low density hemp, blue jeans, mycelium, wood fiber board, cork brick interior cladding, bamboo board, MgO interior sheathing, compressed earth block, cross-laminated timber (CLT), molded cork interior cladding, bamboo wall covering, cork flooring, and recycled rubber flooring.

For these 24 bio-based building materials, the density varied from 8 kg/m$^3$ to 1907 kg/m$^3$. The measured heat capacity from 30 °C to 75 °C was in the range of 0.56 to 3.36 J/(g·°C). For most of materials, increasing the temperature from 10 °C to 38 °C increased their thermal conductivities except for bamboo board, recycled rubber flooring, and MgO interior sheathing. The thermal conductivities of the samples increased slightly as RH increased, with the exception of the MgO interior cladding, which had a decrease in thermal conductivity. Based on water vapor transmission measurements, high density hemp, low density hemp, hemp batt, low density sheep wool and medium density sheep wool were very permeable bio-based building materials.

The sorption isotherms of the bio-based materials tested are highly variable depending on their base material sources and structures. Sheep wool is the most adsorptive, while rubber is the least. Most of them are as water absorptive as traditional wood materials such as OSB and plywood and more absorptive than materials of inorganic bases such as the gypsum board and cement board. Extra caution needs to be taken when applying them in building envelopes to avoid mold or deformation under moist conditions.

## 5. REFERENCES


Architecture 2030, A. Retrieved August 12th 2023 from https://architecture2030.org/why-the-building-sector/

ASTM Standard C1058-03, *Standard Practice for Selecting Temperatures for Evaluating and Reporting Thermal Properties of Thermal Insulation*, ASTM International, West Conshohocken, PA, 2010.

ASTM Standard C303-21*, Standard Test Method for Dimensions and Density of Preformed Block and Board-Type Thermal Insulation*, ASTM International, West Conshohocken, PA, 2021.

ASTM Standard C518-21, *Standard Test Method for Steady-State Thermal Transmission Properties by Means of the Heat Flow Meter Apparatus,* ASTM International, West Conshohocken, PA, 2021.

ASTM Standard E104-20a, Standard *Practice for Maintaining Constant Relative Humidity by Means of Aqueous Solutions,* ASTM International, West Conshohocken, PA, 2020.

ASTM Standard C1498-04a, *Standard Test Method for Hygroscopic Sorption Isotherms of Building Materials,* ASTM International, West Conshohocken, PA, 2016.

ASTM Standard E1269-1, *Standard Test Method for Determining Specific Heat Capacity by Differential Scanning Calorimetry,* ASTM International, West Conshohocken, PA, 2018.

ASTM Standard E96-22, *Standard Test Methods for Gravimetric Determination of Water Vapor Transmission Rate of Materials,* ASTM International, West Conshohocken, PA, 2022.

Glass, S. V., Boardman, C. R., Farkas, N., Lazarcik, E. Q. D., & Zelinka, S. L., 2024. Improved engineering model for water absorption in softwoods. *Science and Technology for the Built Environment*, 1-15. https://doi.org/10.1080/23744731.2023.2299167

UNFCCC, 2015. *Paris Agreement: Decision 1/CP.17 - UNFCCC Document FCCC/CP/2015/L.9/Rev.1* Paris Climate Change Conference, http://unfccc.int/resource/docs/2015/cop21/eng/l09r01.pdf